

See discussions, stats, and author profiles for this publication at: <https://www.researchgate.net/publication/263947962>

# Effects of Inherent Metals on NO Reduction by Coal Char

ARTICLE *in* ENERGY & FUELS · DECEMBER 2011

Impact Factor: 2.79 · DOI: 10.1021/ef201323j

---

CITATIONS

10

---

READS

12

6 AUTHORS, INCLUDING:



Juwei Zhang

IHI Corporation

22 PUBLICATIONS 179 CITATIONS

SEE PROFILE



Shaozeng Sun

Harbin Institute of Technology

45 PUBLICATIONS 367 CITATIONS

SEE PROFILE



Yijun Zhao

Harbin Institute of Technology

13 PUBLICATIONS 145 CITATIONS

SEE PROFILE

# Effects of Inherent Metals on NO Reduction by Coal Char

Juwei Zhang,<sup>\*,†</sup> Shaozeng Sun,<sup>‡</sup> Yijun Zhao,<sup>‡</sup> Xidong Hu,<sup>‡</sup> Guangwen Xu,<sup>†</sup> and Yukun Qin<sup>‡</sup>

<sup>†</sup>State Key Laboratory of Multiphase Complex System, Institute of Process Engineering, Chinese Academy of Sciences, P.O. Box 353, Beijing 100190, P.R. China

<sup>‡</sup>Combustion Engineering Research Institute, School of Energy Science and Engineering, Harbin Institute of Technology, 92 West Dazhi Street, Harbin 150001, P.R. China

**ABSTRACT:** Five coal chars were prepared in a flat flame flow reactor (FFR) which can simulate the temperature and gas composition of a real pulverized coal combustion environment. Reactivity of these chars with NO in the temperature range of 1273–1573 K has been characterized by experiments in a high-temperature drop tube furnace (DTF). Two normalized parameters ( $\bar{X}$  and  $m_c$ ) are proposed to analyze the effect of inherent metal content on char reactivity. The inherent metal catalysts in chars, such as magnesium, potassium, sodium, calcium, and iron, can significantly increase reactivity of char by reducing the activation energy. The reactivity of NO–char reaction increases with  $m_c$  value monotonously and linearly in a certain range. Experimental results showed that the catalytic activity of magnesium, potassium, sodium, calcium, and iron at the temperatures of 1273–1573 K were in decreasing sequence. In this study, the magnesium, which was rarely studied in other literature, appears to have a great catalytic effect on the reduction of NO by chars.

## 1. INTRODUCTION

A considerable amount of work has been conducted on the reaction of NO with chars because of its importance in producing or reducing NO emissions from combustion systems such as fluidized bed or pulverized coal combustion boiler.<sup>1–8</sup> According to previous studies, the catalytic effect of inherent metal in char on the NO–char reaction cannot be ignored, and the catalytic effect of alkali, alkali earth metals, and some first-series transition metals (Fe, Cu, Cr, Co, Ni) is an important aspect in understanding the NO–char reaction.

Illan-Gomez et al.<sup>9–13</sup> studied the catalytic effects of a series of metals (K, Ca, Fe, Cr, Co, Ni, and Cu) on NO reduction in a fixed-bed flow reactor at the temperatures of 573–873 K and found that all these metals catalyzed the reaction to some degree and resulted in a decrease in the apparent activation energy. Lopez et al.<sup>5</sup> studied the influence of potassium on the NO–carbon reaction in a quartz, packed-bed reactor at the temperatures of 773–1123 K and found that the effect of potassium was to significantly increase the reactivity by both increasing the number of reaction sites and reducing the activation energy. Zhong et al.<sup>3,14</sup> studied the catalytic effect of KOH and NaOH on the reaction of NO with char in a drop tube furnace (DTF) at the temperatures of 1173–1523 K and found that KOH could increase the frequency factor and reduce the activation energy of the reduction of NO by char. They also reported that the catalytic activity of KOH was slightly better than that of NaOH.

Most authors<sup>3,5,9–15</sup> studied the catalytic effect of metals on the reaction of NO with chars by demineralization and impregnation to quantify the decrease of the reaction rate. However demineralization was never complete, so the comparison between the catalysts' effect was only between the materials with "higher" and "lower" catalyst loading.<sup>16</sup> In this study, demineralization and impregnation was not used. Instead, a new analysis method was suggested to distinguish catalytic effects of single metals on NO reduction although different catalytic metals were coexistent

in chars. The purpose of this study is to investigate the catalytic effect of inherent metal in chars on NO reduction by different chars in the temperature regime of 1273–1573 K.

## 2. EXPERIMENTAL SECTION

**Char Preparation.** Five Chinese coals, a lignite (YB coal), two bituminous coals (SH coal and SJ coal), and two anthracite coals (YQ coal and JC coal) were used. The raw coals were milled and sieved to ensure that almost all coal particles were in the size of 53–75  $\mu\text{m}$ . The chars were prepared from these coals in a flat flame flow reactor (FFR) as in the previous papers.<sup>17,18</sup> The FFR uses the hot products of the  $\text{CH}_4/\text{CO}/\text{O}_2/\text{N}_2$  combustion flame (1952 K) to heat the char particles, closely approximating the temperature and gas composition of a real pulverized coal combustion environment.<sup>19</sup> Coal particles were pyrolyzed in a postflame zone of the flat flame operated under fuel-rich conditions (Equivalence ratio  $\phi = 1.4$ ), so that this experiment would be more representative of the fuel-rich region in a coal flame than experiments conducted in inert gases, such as nitrogen or argon.<sup>19,20</sup> The maximum particle heating rate in the FFR was  $10^5$  K/s. The feeding rate of coal particles was 4–6 g/h, depending on the bulk density of coals. This low feeding rate minimizes the interaction between particles to ensure single particle reaction behavior. The particle residence time in this experiment was around 60 ms which ensured that the devolatilization process was completed in the postflame zone in FFR.<sup>21</sup>

**Experiment in DTF.** Experiments were conducted in a high-temperature, laminar drop tube furnace (DTF). A schematic of the DTF is shown in Figure 1. The flow reactor is an alumina tube with an inner diameter of 50 mm and a length of 1.4 m, which was heated electrically to the required temperature before every experiment. The furnace temperatures in experiments were set to 1273, 1373, 1473, and 1573 K, respectively. Char particles were entrained by  $\text{N}_2$  (0.5 L/min, 1 atm, 273 K)

**Received:** September 5, 2011

**Revised:** November 8, 2011

**Published:** November 17, 2011

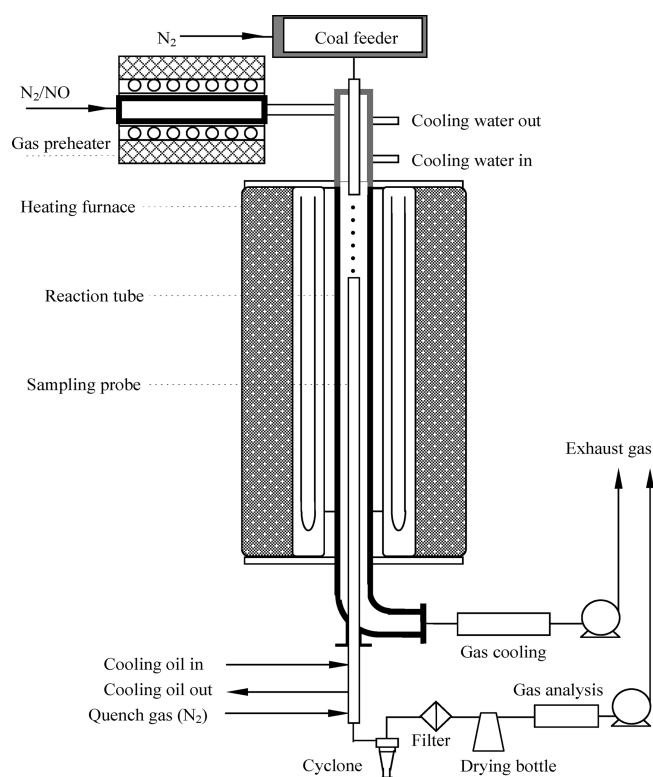


Figure 1. Schematic diagram of DTF facility.

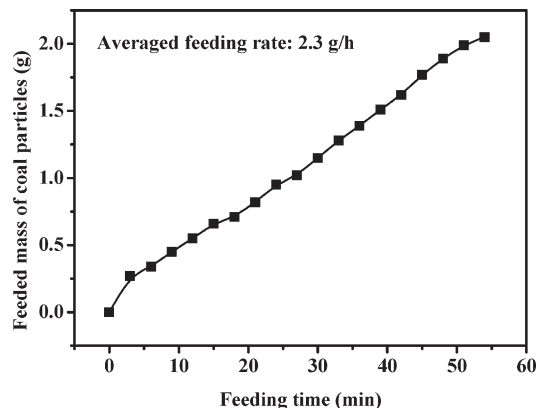


Figure 2. Calibration curve of particle feeder.

into the furnace at a feeding rate of about 5–20 g/h depending upon the bulk density of chars. A gas flow (5 L/min, 1 atm, 273 K) consisting of NO and N<sub>2</sub> was preheated to 873 K before being introduced into the hot zone of the furnace. The initial NO concentration was set to 1040 ppmv. Reaction products were sampled by an oil-cooled, nitrogen-quenched probe, and the compositions of exhaust gases were measured by an online Fourier transform infrared (FTIR) gas analyzer (GASMET-DX4000, Finland). The sampling point was fixed to the position 600 mm away from the injection port, and the residence time was 2.23–2.75 s depending upon temperatures.

It is well-known that the presence of H<sub>2</sub>O in the sample gas can influence the precision of FTIR due to its spectrum interference, fortunately, there is almost no H<sub>2</sub>O in the gas in our experiments. As for the repeatability of these experiments, we just did several replicate experiments to validate the experiments results, since this kind of experiment is

Table 1. Ultimate and Proximate Analyses of Chars

| sample  | ultimate analysis (daf, %) |     |     |     | proximate analysis (db, %) |      |      |
|---------|----------------------------|-----|-----|-----|----------------------------|------|------|
|         | C                          | H   | N   | S   | VM                         | ash  | FC   |
| YB char | 92.1                       | 3.6 | 1.0 | 1.5 | 14.2                       | 31.3 | 54.5 |
| YQ char | 94.1                       | 2.2 | 1.3 | 1.8 | 5.8                        | 11.6 | 82.5 |
| JC char | 97.1                       | 1.0 | 1.2 | 0.5 | 6.4                        | 6.1  | 87.9 |
| SJ char | 93.9                       | 2.5 | 1.5 | 1.6 | 9.3                        | 56.4 | 34.3 |
| SH char | 92.6                       | 2.3 | 0.9 | 1.4 | 11.1                       | 10.6 | 78.3 |

Table 2. Ash Content Analyses of Chars

| sample  | ash content (wt %) |                                |      |     |                  |                   |                  |                                |                 |
|---------|--------------------|--------------------------------|------|-----|------------------|-------------------|------------------|--------------------------------|-----------------|
|         | SiO <sub>2</sub>   | Fe <sub>2</sub> O <sub>3</sub> | CaO  | MgO | K <sub>2</sub> O | Na <sub>2</sub> O | TiO <sub>2</sub> | Al <sub>2</sub> O <sub>3</sub> | SO <sub>3</sub> |
| YB char | 50.5               | 13.3                           | 7.0  | 1.3 | 2.3              | 2.3               | 0.5              | 16.3                           | 6.1             |
| YQ char | 47.1               | 6.6                            | 4.0  | 1.4 | 2.7              | 2.3               | 0.9              | 32.4                           | 0.9             |
| JC char | 37.5               | 13.3                           | 1.9  | 0.8 | 1.2              | 1.5               | 2.1              | 34.5                           | 7.1             |
| SJ char | 56.0               | 4.2                            | 3.1  | 1.0 | 3.0              | 1.8               | 0.7              | 30.0                           | 1.7             |
| SH char | 30.2               | 22.5                           | 21.3 | 1.0 | 2.0              | 3.0               | 0.4              | 11.6                           | 7.7             |

Table 3. Analysis of Chars' Physical Properties

| sample  | physical analysis       |   |          |                         |                                    |
|---------|-------------------------|---|----------|-------------------------|------------------------------------|
|         | BET (m <sup>2</sup> /g) | Hg <sub>20</sub> <sup>a</sup> (m <sup>2</sup> /g) | porosity | mass mean diameter (μm) | true density (k gm <sup>-3</sup> ) |
| YB char | 217.7                   | 18.2  | 0.845    | 52.9                    | 2215                               |
| YQ char | 26.2                    | 2.0   | 0.557    | 46.5                    | 1833                               |
| JC char | 2.81                    | 1.94  | 0.6      | 31.2                    | 2172                               |
| SJ char | 70.0                    | 6.9   | 0.746    | 50.8                    | 2065                               |
| SH char | 244.4                   | 11.1  | 0.784    | 53.3                    | 1586                               |

<sup>a</sup> The specific surface area of pores larger than 20 nm.

very time-consuming and expensive. The good repetition of the results is mainly associated with the good precision of gas composition measurement and steady coal particle feeding, which were well ensured in this study. The error range of FTIR is ±2% and the stability of particle feeding can be inferred from the good linear relationship of calibration curve of particle feeder (see Figure 2).

**Characterization Measurements of Coal and Char.** Table 1 gives the results of the proximate and ultimate analyses. Table 2 and Table 3 list the analysis results of char ash content (PRC National Standard GB/T 1574-2007) and physical properties, respectively. The complete pore structure for all char samples was obtained by combining porosimetry with gas adsorption. Macropore/mesopore surface area and pore volume were measured by mercury porosimetry (Autopore II 9220, Micromeritics, Norcross, GA). Nitrogen adsorption at 77 K was performed in an automated adsorption analyzer (ASAP 2020, Micromeritics, Norcross, GA) and the specific surface area was calculated by the Brunauer–Emmett–Teller (BET) equation. The true density was measured by a helium pycnometer (AccuPyc 1330, Micromeritics, Norcross, GA). The mass mean diameter ( $D_{4,3}$ ) of char particles was estimated by a laser size analyzer (Master Min, Malvern, UK). The results are also given in Table 3.

### 3. RESULTS AND DISCUSSION

**Determination of the Char Reactivity.** According to the previous studies, the reaction of NO with coal char is found to be

of first order with respect to NO.<sup>22–24</sup> Based on our previous study,<sup>18</sup> the intrinsic rate constant or the intrinsic reactivity of char ( $\text{mol m}^{-2} \text{s}^{-1} \text{Pa}^{-1}$  or  $\text{mol m}^{-2} \text{s}^{-1} \text{atm}^{-1}$ ) can be expressed as

$$k = -\ln(1-x)/(\eta Y A m t R T) \quad (1)$$

where  $x$  is the NO conversion,  $\eta$  is the effectiveness factor,  $Y$  is the mass fraction of carbon in the char particle considering the contribution of ash to the total surface area and only the carbon surface is reactive,  $A$  is the specific internal area of char ( $\text{m}^2 \text{g}^{-1}$ ),  $m$  is the char mass per unit volume of furnace ( $\text{g m}^{-3}$ ),  $t$  is the residence time of char particles (s),  $R$  is the gas constant ( $\text{J mol}^{-1} \text{K}^{-1}$ ), and  $T$  is the temperature (K). The specific internal surface area of char particle  $A$  can be measured by mercury porosimetry or nitrogen adsorption. Based on our previous study<sup>18</sup> and other studies,<sup>25,26</sup> in comparison to the BET surface area (measured by nitrogen adsorption), the Hg surface area (measured by mercury porosimetry) is a better basis for normalizing the reactivity of different coal chars due to less scattering of the measured values. So the Hg surface area is used to represent the specific internal surface area of the char particle.

As in eq 1,  $k$  is a pseudoconstant whose value depends on  $T$ , and the influence of  $T$  variations on  $RT$  is negligible compared with that on  $k$ . Therefore, the values of  $k$  can be presented in Arrhenius plots as straight lines. Then  $k$  can be expressed in Arrhenius form as follows:

$$k = k_0 \exp(-E/RT) \quad (2)$$

If  $-r_{\text{NO}}$  is expressed in terms of NO molar concentration  $C_{\text{NO}}$  ( $\text{mol m}^{-3}$ )

$$-r_{\text{NO}} = \eta k' Y A m C_{\text{NO}} \quad (3)$$

and the intrinsic rate coefficient  $k'$  is in  $\text{m/s}$

$$\eta k' = -\ln(1-x)/(Y A m t) \quad (4)$$

thus,

$$k' = k R T \quad (5)$$

The effectiveness factor  $\eta$  is the ratio of the actual reaction rate to the rate attainable if no pore diffusion resistance existed

$$\eta = 3(1/\tan \phi - 1/\phi)/\phi \quad (6)$$

where  $\phi$  is the Thiele modulus

$$\phi = d_p \sqrt{k' \rho_p Y A / D_e} \quad (7)$$

where  $\rho_p$  is the apparent density of char ( $\text{m}^3 \text{g}^{-1}$ ) and  $D_e$  is the effective diffusion coefficient ( $\text{m}^2 \text{s}^{-1}$ ). Assuming that the bulk and Knudsen diffusion proceed in parallel,  $D_e$  is given by

$$D_e = \varepsilon(1/D_0 + 1/D_k)^{-1}/\tau \quad (8)$$

where  $D_0$  is the molecular diffusion coefficient ( $\text{m}^2 \text{s}^{-1}$ ) and  $D_k$  is the Knudsen diffusion coefficient ( $\text{m}^2 \text{s}^{-1}$ ). The porosity of char particle  $\varepsilon$  can be obtained from

$$\varepsilon = 1 - \rho_p/\rho_t \quad (9)$$

The tortuosity factor  $\tau$  can be obtained through the expression proposed by Wakao and Smith<sup>27</sup>

$$\tau = 1/\varepsilon \quad (10)$$

**Table 4. Effectiveness Factors for the NO–Char Reaction for Five Chars**

| sample  | ash (%) | Hg <sub>20</sub> (m <sup>2</sup> /g) | $\eta_{1273}$ | $\eta_{1373}$ | $\eta_{1473}$ |
|---------|---------|--------------------------------------|---------------|---------------|---------------|
| YB char | 31.3    | 18.2                                 | 0.895         | 0.849         | 0.744         |
| SH char | 10.6    | 11.1                                 | 0.966         | 0.916         | 0.869         |
| SJ char | 56.4    | 6.9                                  | 0.963         | 0.951         | 0.914         |
| YQ char | 25.6    | 2.0                                  | 0.982         | 0.970         | 0.933         |
| JC char | 6.10    | 1.94                                 | 0.995         | 0.986         | 0.975         |

The Knudsen diffusion coefficient  $D_k$  can be expressed as

$$D_k = 2r_e \sqrt{8RT_p/(\pi M_{\text{NO}})}/3 \quad (11)$$

where  $r_e$  is an empirical mean pore radius (m) according to the pore model proposed by Satterfield<sup>28</sup> and can be defined as

$$r_e = 2\varepsilon/(A_i \rho_p) \quad (12)$$

The value of  $k$  or  $k'$  can be obtained from eqs 1, 4, 6, and 7 by trial and error. The procedure of “trial and error” is: (1) assuming a value of effectiveness factor  $\eta'$ ; (2) determining  $k'$  with  $\eta'$  by eq 4; (3) determining a new  $\eta$  value with  $k'$  by eq 6 and 7; (4) repeating step 1, 2, 3, 4 until  $\eta = \eta'$ , then the true  $\eta$  value can be obtained. Finally, according to the theories mentioned above, the kinetic parameters of the NO–char reaction can be obtained.

Obtaining effectiveness factor  $\eta$  is the key step for determining intrinsic reactivity  $k$ . The calculated values of  $\eta$  at various temperatures for five chars are listed in Table 4. The ash content and Hg surface area are also given. It can be seen that the values of  $\eta$  are in the range of 0.690–0.995 and above 0.9 in most conditions, indicating low diffusion limitation for NO–char reaction in this study. On the other hand, the values of  $\eta$  are almost all increased with the decreasing of Hg surface area of char but have no regular correlation with ash content, further indicating low external diffusion limitation in ash layer.

**Effect of the Inherent Metal.** Illan-Gomez et al.<sup>10–14</sup> studied the effects of metal (K, Ca, Fe, Cu, Cr, Co, Ni) on the reaction of NO with carbon and found that the catalytic activity in the decreasing sequence was of K, Fe, Co, and Ni ( $T < 673 \text{ K}$ ), and of K, Co, Ni, and Cu ( $T > 773 \text{ K}$ ), with potassium showing the highest catalytic activity in the whole temperature range (the highest temperature is 1173 K).<sup>3</sup> Chen<sup>29</sup> found that the NO reduction capacity of Pittsburgh #8 coal char was obviously improved by impregnating the char with a  $\text{Ca}(\text{OH})_2$  solution (the content of  $\text{Ca}(\text{OH})_2$  in the char was increased from 2.97% to 5.21%). Zhong et al.<sup>3</sup> studied the alkali metal oxides catalytic effects on the reaction of NO with char by impregnation and further verified that potassium and sodium hydroxides (KOH and NaOH) could promote the reduction of NO with char. Further study<sup>15</sup> in a DTF at the temperatures of 1173–1323 K proved that the benefit of increasing the KOH content in the char particles decreased when there was more than 1.0 wt % of the catalyst in the char.

Some conclusions above can also be further confirmed by the experimental results in this study. The catalytic effects of different metals on the reaction of chars with NO are shown in Figure 3 where the molar ratios of metal to corresponding fixed carbon are plotted versus char reactivity  $k$  at the temperatures of 1273–1573 K. The molar ratio of metal to fixed carbon is used to normalize the differences of carbon content in different chars. The correlation factors for linear least-squares estimation are also listed in Table 5 which shows that metal catalysts have a great catalytic effect on the reactivity of chars with NO. It deserves

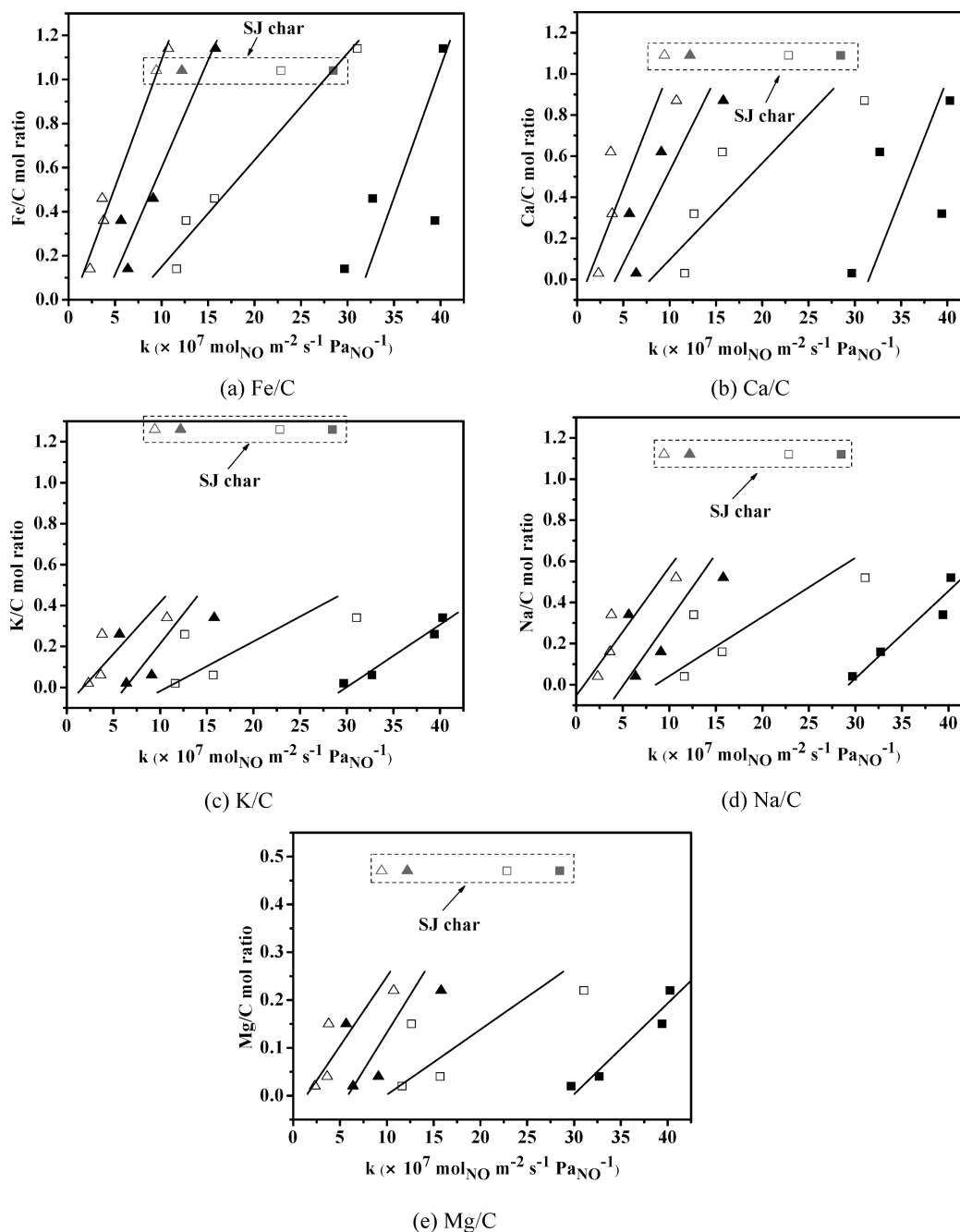


**Figure 3.** Molar ratio of metal to corresponding fixed carbon for five chars versus reaction rate toward NO (the data of SJ char is excluded in the linear fit,  $\Delta$  1273 K,  $\blacktriangle$  1373 K,  $\square$  1473 K,  $\blacksquare$  1573 K).

noting that the data of SJ char is not included in the linear fit for its high ash content (its data are enclosed in a rectangular box in Figure 3). The ash content in SJ char (56.4 wt %) is much higher than that in other chars (see Table 1). At high temperature the pores of char can be blocked by melting ash and some catalytically metal components in the char are also partly transformed into less active components, such as potassium silicates. The ash itself can hinder the contact between the char and NO. Figure 3 shows that SJ char has the lowest reactivity at temperature 1573 K though the ratios of K/C, Na/C, Ca/C, and Mg/C in SJ char are all higher than that in other chars.

To take into account the influences of the concentration differences of metal catalysts in different chars on NO—char reaction, a normalized correlation factor  $X$  is proposed:

$$X = R^2/M \quad (13)$$

where  $R^2$  is the correlation factor and  $M$  is the molar ratio of metal to fixed carbon; both of the parameters and their averaged values are listed in Table 5. The high value of  $\bar{X}$  (average of  $X$  at different temperatures) indicates great influence of the metal. It can be seen from Table 5 that the catalytic activity of per unit metal in the decreasing sequence is of Mg, K, Na, Ca, and Fe.

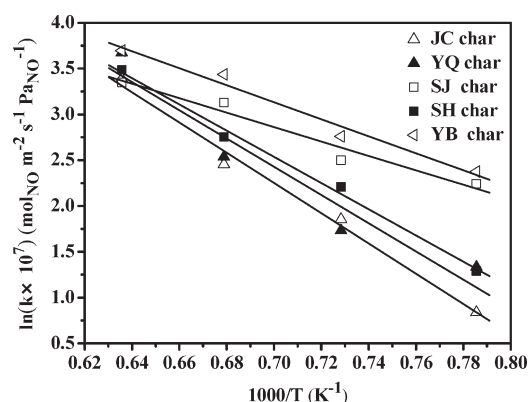


**Table 5. Correlation Factors between Metal Content and Reactivity at Different Temperatures**

| metal | 1273 K                |  | 1373 K                |  | 1473 K                |  | 1573 K                |  | averaged values       |           | <i>M</i> |
|-------|-----------------------|--|-----------------------|--|-----------------------|--|-----------------------|--|-----------------------|-----------|----------|
|       | <i>R</i> <sup>2</sup> | <i>X</i> <sub><i>T</i><sub>1</sub></sub> | <i>R</i> <sup>2</sup> | <i>X</i> <sub><i>T</i><sub>2</sub></sub> | <i>R</i> <sup>2</sup> | <i>X</i> <sub><i>T</i><sub>3</sub></sub> | <i>R</i> <sup>2</sup> | <i>X</i> <sub><i>T</i><sub>4</sub></sub> | <i>R</i> <sup>2</sup> | $\bar{X}$ |          |
| Mg    | 0.86                  | 7.82                                     | 0.65                  | 5.91                                     | 0.76                  | 6.91                                     | 0.96                  | 8.73                                     | 0.81                  | 7.53      | 0.11     |
| K     | 0.81                  | 4.76                                     | 0.58                  | 3.41                                     | 0.70                  | 4.12                                     | 0.98                  | 5.76                                     | 0.77                  | 4.50      | 0.17     |
| Na    | 0.88                  | 3.38                                     | 0.71                  | 2.73                                     | 0.81                  | 3.12                                     | 0.96                  | 3.69                                     | 0.84                  | 3.21      | 0.26     |
| Ca    | 0.83                  | 1.80                                     | 0.87                  | 1.89                                     | 0.86                  | 1.87                                     | 0.62                  | 1.35                                     | 0.79                  | 1.74      | 0.46     |
| Fe    | 0.99                  | 1.87                                     | 0.96                  | 1.81                                     | 0.99                  | 1.87                                     | 0.71                  | 1.34                                     | 0.91                  | 1.72      | 0.53     |

**Table 6. Summary of Activation Energies for NO—Char Reaction**

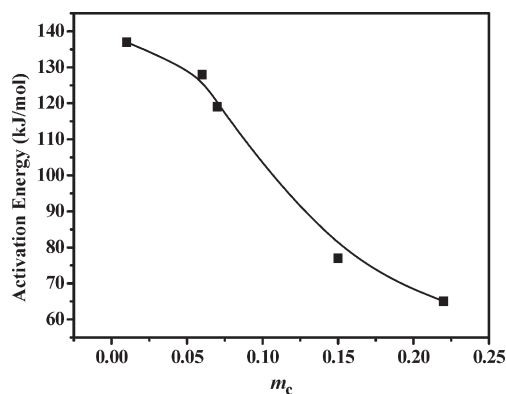
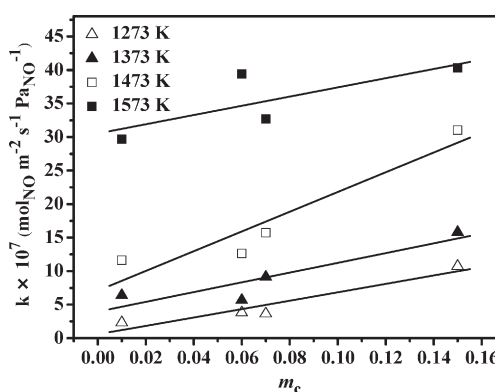
| sample  | ash (%) | <i>E</i> (kJ/mol) | <i>m</i> <sub>c</sub> |
|---------|---------|-------------------|-----------------------|
| YB char | 31.3    | 77                | 0.15                  |
| YQ char | 25.6    | 128               | 0.06                  |
| JC char | 6.1     | 137               | 0.01                  |
| SJ char | 56.4    | 65                | 0.22                  |
| SH char | 10.6    | 119               | 0.07                  |

**Figure 4.** Arrhenius plots of NO—char reactions for five chars.

The catalytic effect of potassium is found to be better than sodium, which is also observed in other literature. The catalytic activity of Fe is almost the same as Ca. Although Mg is less studied in other literature due to its low concentration in both coals and chars, it appears to have a relatively greater catalytic effect on the reduction of NO with chars, which indicates that the catalytic effect of Mg on the reduction of NO by chars cannot be neglected.

The values of *X* for different temperatures are also presented in Table 5. Although the values of *R*<sup>2</sup> scatter widely in Table 5, the values of *X* have the same sequence as that of  $\bar{X}$ . Therefore  $\bar{X}$  parameter can be used to estimate the catalytic activity of metals.

**Effect of Main Metal Oxides.** Many previous studies<sup>29–32</sup> demonstrated that the existence of metal oxides, such as Fe<sub>2</sub>O<sub>3</sub>, CaO, MgO, K<sub>2</sub>O, and Na<sub>2</sub>O, in ash could catalyze the NO—char reaction. The analysis data of ashes for YB char, YQ char, JC char, SJ char, and SH char show that there are great differences in contents of metal oxides. The content of catalytic metal oxides in ashes can be presented by the sum of the mass fraction of main metal oxides (MMO), i.e., MMO = Fe<sub>2</sub>O<sub>3</sub> + CaO + MgO + K<sub>2</sub>O + Na<sub>2</sub>O. Considering the differences of the fixed carbon concentration

**Figure 5.** Effect of the content of main metal oxides in the char particles on the activation energy.**Figure 6.** Reactivity versus *m*<sub>c</sub> value of five chars.

in chars, a normalized parameter *m*<sub>c</sub> is proposed:

$$m_c = \text{MMO}/\text{FFC} \quad (14)$$

where MMO is the sum of the mass fraction of main metal oxides, and FFC is the mass fraction of fixed carbon of the corresponding char. The calculated results for all chars are listed in Table 6.

Figure 4 shows the Arrhenius plots of all chars. A good linear relationship can be obtained for all cases. The activation energies obtained from Arrhenius plots are also listed in Table 6.

Most researchers observed that the activation energy increases in value at temperatures between 800 and 1000 K. Although there are large variations in the measured activation energies, the values measured generally change from 75 kJ/mol below 950 K and 180 kJ/mol above this temperature.<sup>26,33–35</sup> Illan-Gomez et al.<sup>36</sup> reported an activation energy ranging between 30 and 86 kJ/mol in the low-temperature regime (573–873 K) for the NO—carbon reaction in the presence of different metal catalysts. Lopez et al.<sup>5</sup> studied values of the activation energy for the NO—carbon reaction catalyzed by potassium at temperatures above 923 K and found that the values agreed with the values reported by Illan-Gomez et al. at their highest reported temperature (873 K). In this study, as shown in Table 6, it is also observed that the activation energies obtained from different chars range from 65 to 137 kJ/mol. The current values are slightly higher than that reported by Illan-Gomez et al. and Lopez et al. Generally, the values of activation energy decrease with the increase of ash content because more ash means more catalytic matter in the char.

However, the activation energy value of YQ char is almost equal to that of SH char although the ash content in YQ char is almost twice as high as that in SH char. A reasonable explanation can be obtained if  $m_c$  values are compared. The  $m_c$  value of YQ char is almost equal to that of SH char. In Figure 5, the apparent activation is plotted versus  $m_c$ , and it displays explicitly that the presence of catalytic metal significantly decreases the apparent activation energy of the NO—char reaction.

Figure 6 shows the experimental data concerning the effects of metal oxides on the NO reduction. The SJ char is also not presented in Figure 6 for its higher ash content. The increase of the catalytic metal content can noticeably accelerate the reduction of NO by chars. The reactivity of NO—char reaction increases with  $m_c$  value almost linearly.

#### 4. CONCLUSIONS

Five representative coal chars were prepared in a FFR which simulated a real pulverized coal combustion environment. A study of the effects of the inherent catalytic metals in char on the activation energy and reactivity of char for NO—char reaction has been conducted in a DTF in the temperature range of 1273–1573 K. It is known that the metals with different forms and dispersion nature have different catalytic activities, however, we have to confess that we can only study them in a “black box”, as it is too complicated and impossible to take these factors into account. Fortunately, we have obtained some valuable conclusions as follows.

K, Na, Ca, Mg, and Fe are proved to be very effective catalysts for NO reduction by chars. A normalized correlation factor  $\bar{X}$  is proposed to analyze the effect of metal concentration on char reactivity; the catalytic activity of per unit metal in decreasing sequence is Mg, K, Na, Ca, and Fe at temperatures of 1273–1573 K. It should be noticed that Mg has significant catalytic activity although its content in chars is very low, which is less studied in other literature.

The activation energies obtained from different chars range from 65 to 137 kJ/mol, the scattering of which is due to the existence of metal catalysts. The effect of metal catalysts is to significantly increase the char reactivity by reducing the activation energy. A normalized parameter  $m_c$  is proposed to analyze the effect of the main metal oxide content on the char reactivity. The increase of the main metal oxide content noticeably accelerates the reduction of NO by char particles linearly.

#### AUTHOR INFORMATION

##### Corresponding Author

\*Tel.: +86 10 82544905. E-mail: jwzhang@home.ipe.ac.cn.

#### ACKNOWLEDGMENT

We are grateful for the financial support of the National High Technology Research and Development of China (contract 2009-AA02Z209), Natural Science Foundation of China (contract 21006110), and Key Projects in the National Science & Technology Pillar Program (contract 2009BAC64B05).

#### REFERENCES

- (1) Smoot, L. D.; Hill, S. D.; Xu, H. *Prog. Energy Combust. Sci.* **1998**, 24 (5), 385–408.
- (2) Jiang, X. M.; Zheng, C. G.; Yan, C.; Liu, D. C.; Qiu, J. R.; Li, J. B. *Fuel* **2002**, 81 (6), 793–797.
- (3) Zhong, B. J.; Zhang, H. S.; Fu, W. B. *Combust. Flame* **2003**, 132 (3), 364–373.
- (4) Gu, M. Y.; Zhang, M. C.; Fan, W. D.; Wang, L.; Tian, F. G. *Fuel* **2005**, 84 (6), 2093–2101.
- (5) Lopez, D.; Calo, J. *Energy Fuels* **2007**, 21 (4), 1872–1878.
- (6) Xie, G. L.; Fan, W. D.; Song, Z. L.; Lu, J.; Yu, J.; Zhang, M. C. *Energy Fuels* **2007**, 21 (6), 3134–3143.
- (7) Cancès, J.; Commandré, J. M.; Salvador, S.; Dagaut, P. *Fuel* **2008**, 87 (3), 274–289.
- (8) Li, Z. Q.; Jing, J. P.; Chen, Z. C.; Ren, F.; Xu, B.; Wei, H. D.; Ge, Z. H. *Combust. Sci. Technol.* **2008**, 180 (7–9), 1370–1394.
- (9) Illan-Gomez, M. J.; Linares-Solano, A.; Radovic, L. R.; Salinas-Martinez, D. L. C. *Energy Fuels* **1995**, 9 (1), 97–103.
- (10) Illan-Gomez, M. J.; Linares-Solano, A.; Radovic, L. R.; Salinas-Martinez, D. L. C. *Energy Fuels* **1995**, 9 (1), 112–118.
- (11) Illan-Gomez, M. J.; Linares-Solano, A.; Radovic, L. R.; Salinas-Martinez, D. L. C. *Energy Fuels* **1995**, 9 (3), 540–548.
- (12) Illan-Gomez, M. J.; Linares-Solano, A.; Salinas-Martinez, D. L. C. *Energy Fuels* **1995**, 9 (6), 976–983.
- (13) Illan-Gomez, M. J.; Linares-Solano, A.; Salinas-Martinez, D. L. C. *Energy Fuels* **1996**, 10 (1), 158–168.
- (14) Zhong, B. J.; Tang, H. *Combust. Flame* **2007**, 149 (1–2), 234–243.
- (15) Akira, T.; Takayuki, T.; Yasukatsu, T. *Fuel* **1983**, 62 (1), 62–68.
- (16) Aarna, I.; Suuberg, E. M. *Energy Fuels* **1999**, 13 (6), 1145–1153.
- (17) Sun, S. Z.; Zhang, J. W.; Hu, X. D.; Wu, S. H.; Yang, J. C.; Wang, Y.; Qin, Y. K. *Energy Fuels* **2009**, 23 (1), 74–80.
- (18) Zhang, J. W.; Sun, S. Z.; Hu, X. D.; Sun, R.; Qin, Y. K. *Energy Fuels* **2009**, 23 (5), 2376–2382.
- (19) Zeng, D.; Clark, M.; Gunderson, T.; Hecker, W. C.; Fletcher, T. H. *Proc. Combust. Inst.* **2005**, 30, 2213–2221.
- (20) Fletcher, T. H.; Ma, J. L.; Rigby, J. R.; Brown, A. L.; Webb, B. W. *Prog. Energy Combust. Sci.* **1997**, 23 (3), 293–301.
- (21) Ma, J. L. Ph.D. Thesis, Brigham Young University, Utah, 1996.
- (22) Song, Y. H.; Beer, J. M.; Sarofim, A. F. *Combust. Sci. Technol.* **1981**, 25, 237–240.
- (23) Aarna, I.; Suuberg, E. M. *Fuel* **1997**, 76 (6), 475–491.
- (24) Schonenbeck, C.; Gadiou, R.; Schwartz, D. *Fuel* **2004**, 83 (4), 443–450.
- (25) Commandre, J. M.; Stanmore, B. R.; Salvador, S. *Combust. Flame* **2002**, 128 (3), 211–216.
- (26) Salvador, S.; Commandre, J. M.; Stanmore, B. R.; Gadiou, R. *Energy Fuels* **2004**, 18 (2), 296–301.
- (27) Wakao, N.; Smith, J. M. *Chem. Eng. Sci.* **1962**, 17 (11), 825–837.
- (28) Satterfield, C. N. *Mass Transfer in Heterogeneous Catalysis*; MIT Press: Cambridge, MA, 1970.
- (29) Chen, W. Y.; Ma, L. *AIChE J.* **1996**, 42 (7), 1968–1976.
- (30) Hansen, P. F. B. K.; Dam-Johansen, Johnsson, J. E.; Hulgaard, T. *Chem. Eng. Sci.* **1992**, 47 (9–11), 2419–2424.
- (31) Garcia-Garcia, A.; Illan-Gomez, M. J.; Linares-Solano, A.; Salinas-Martinez, D. L. C. *Fuel* **1997**, 76 (6), 499–505.
- (32) Ohtsuka, Y.; Wu, Z.; Furimsky, E. *Fuel* **1997**, 76 (14–15), 1361–1367.
- (33) Chan, L. K.; Sarofim, A. F.; Beer, J. M. *Combust. Flame* **1983**, 52, 37–45.
- (34) Suuberg, E. M.; Teng, H.; Calo, J. M. *Proc. Combust. Inst.* **1990**, 23, 1199–1205.
- (35) Akira, T. L.; Yoshiaki, O.; Takaaki, K.; Yasukatsu, T. *Fuel* **1979**, 58 (8), 614–618.
- (36) Illan-Gomez, M. J.; Linares-Solano, A.; Salinas-Martinez, D. L. C.; Calo, J. M. *Energy Fuels* **1993**, 7 (1), 146–154.